AD-A060 370 AIR FORCE AERO PROPULSION LAB WRIGHT-PATTERSON AFB OHIO F/G 10/3

SOME FATIGUE CHARACTERISTICS OF NICKEL BATTERY PLAQUE.(U)

JUL 78 D H FRITTS

UNCLASSIFIED AFAPL-TR-78-37 NL

1 OF 1

AD
A060370

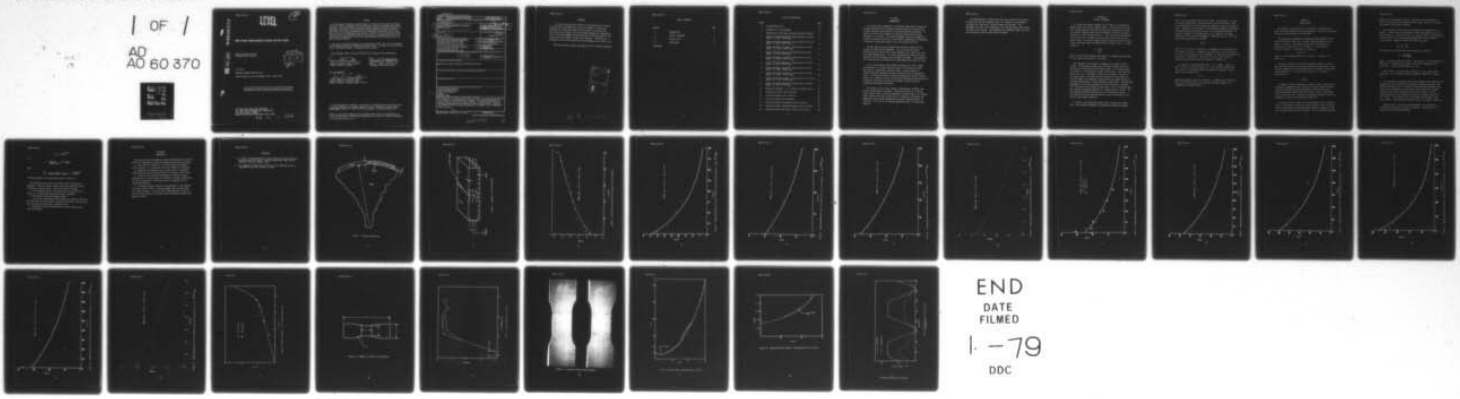

END
DATE
FILMED
1-79
DDC

AFAPL-TR-78-37

LEVEL II

AD A060370

DDC FILE COPY

SOME FATIGUE CHARACTERISTICS OF NICKEL BATTERY PLAQUE

Energy Conversion Branch
Aerospace Power Division

DDC
RECEIVED
OCT 26 1978
F

July 1978

TECHNICAL REPORT AFAPL-TR-78-37

Interim Report for Period November 1977 - April 1978

Approved for public release; distribution unlimited.

AIR FORCE AERO PROPULSION LABORATORY
AIR FORCE WRIGHT AERONAUTICAL LABORATORIES
AIR FORCE SYSTEMS COMMAND
WRIGHT-PATTERSON AIR FORCE BASE, OHIO 45433

78 10 16 032

NOTICE

When Government drawings, specifications, or other data are used for any purpose other than in connection with a definitely related Government procurement operation, the United States Government thereby incurs no responsibility nor any obligation whatsoever; and the fact that the government may have formulated, furnished, or in any way supplied the said drawings, specifications, or other data, is not to be regarded by implication or otherwise as in any manner licensing the holder or any other person or corporation, or conveying any rights or permission to manufacture, use, or sell any patented invention that may in any way be related thereto.

This report has been reviewed by the Information Office (OI) and is releasable to the National Technical Information Service (NTIS). At NTIS, it will be available to the general public, including foreign nations.

This technical report has been reviewed and is approved for publication.

DAVID H. FRITTS, Project Engineer
Energy Conversion Branch

DONALD P. MORTEL, Tech Area Mgr
Energengy Conversion Branch

FOR THE COMMANDER

KARL H. MULLER, Lt Colonel, USAF
Deputy Director, Aerospace Power Division

"If your address has changed, if you wish to be removed from our mailing list, or if the addressee is no longer employed by your organization please notify AFAPL/POE-1, *W-PAFB, OH 45433 to help us maintain a current mailing list".*

Copies of this report should not be returned unless return is required by security considerations, contractual obligations, or notice on a specific document.

AIR FORCE/56780/15 September 1978 — 205

UNCLASSIFIED

SECURITY CLASSIFICATION OF THIS PAGE (When Data Entered)

14

REPORT DOCUMENTATION PAGE

READ INSTRUCTIONS BEFORE COMPLETING FORM

1. REPORT NUMBER: AFAPL-TR-78-37

2. GOVT ACCESSION NO.

3. RECIPIENT'S CATALOG NUMBER

9

6

4. TITLE (and Subtitle): SOME FATIGUE CHARACTERISTICS OF NICKEL BATTERY PLAQUE.

5. TYPE OF REPORT & PERIOD COVERED: Technical Report (Interim) rept. November 1977-April 1978,

6. PERFORMING ORG. REPORT NUMBER

10

7. AUTHOR(s): David H. Fritts

8. CONTRACT OR GRANT NUMBER(s): In-House 17 54

9. PERFORMING ORGANIZATION NAME AND ADDRESS: Air Force Aero Propulsion Laboratory, Aerospace Power Division (POE), Wright-Patterson AFB, OH 45433

16

10. PROGRAM ELEMENT, PROJECT, TASK AREA & WORK UNIT NUMBERS: Project 2303, Task 2303S4, Work Unit 2303S402

61102F

11. CONTROLLING OFFICE NAME AND ADDRESS: Air Force Aero Propulsion Laboratory, Aerospace Power Division, Wright-Patterson AFB, OH 45433

11

12. REPORT DATE: July 1978

13. NUMBER OF PAGES

14. MONITORING AGENCY NAME & ADDRESS (if different from Controlling Office)

12 35p.

15. SECURITY CLASS. (of this report): Unclassified

15a. DECLASSIFICATION/DOWNGRADING SCHEDULE

16. DISTRIBUTION STATEMENT (of this Report)

Approved for public release; distribution unlimited.

17. DISTRIBUTION STATEMENT (of the abstract entered in Block 20, if different from Report)

18. SUPPLEMENTARY NOTES

19. KEY WORDS (Continue on reverse side if necessary and identify by block number)

Nickel-Cadmium Batteries
Nickel-Hydrogen Batteries
Nickel-Zinc Batteries
Fatigue
Battery Plaque

20. ABSTRACT (Continue on reverse side if necessary and identify by block number)

The conductance of sintered nickel battery plaque is experimentally determined as the plaque is being mechanically stressed. The plaque was subjected to bonding fatigue tests and to tensile testing. It was found that the plaque conductance exponentially decreases with bonding fatigue cycling. Also, it was determined that the plaque conductance is a function of its instantaneous state of stress.

DD FORM 1 JAN 73 1473 EDITION OF 1 NOV 65 IS OBSOLETE

UNCLASSIFIED

SECURITY CLASSIFICATION OF THIS PAGE (When Data Entered)

011570

LB

FOREWORD

This report describes the variance of the conductivity of battery nickel plaque due to mechanical strain and fatigue. The work was performed in the Aerospace Power Division (POE-1) of the Air Force Aero Propulsion Laboratory, Air Force Wright Aeronautical Laboratories, Air Force Systems Command, Wright-Patterson Air Force Base, Ohio, under Project 2303, Task 2303S4, and Work Unit 2303S402. The effort was conducted by David Fritts during the period November 1977 to April 1978.

The author wishes to thank John Leonard for his valuable assistance.

ACCESSION for
NTIS White Section ☑
DDC Buff Section ☐
UNANNOUNCED ☐
JUSTIFICATION
BY
DISTRIBUTION/AVAILABILITY CODES
Dist. SPECIAL
A

78 10 16 032

TABLE OF CONTENTS

SECTION		PAGE
I	INTRODUCTION	1
II	FATIGUE IN BENDING	3
III	TENSILE TESTS	5
IV	CONCLUSIONS	8
REFERENCES		9

LIST OF ILLUSTRATIONS

FIGURE		PAGE
1	Fatigue Bonding Test	10
2	Schematic of Failed Specimen	11
3	Characteristic Resistance Increase with Cyclic Bonding	12
4	Sponge Conductance of 30-mil Plaque Cycled on 5.5-Inch Arbor; $G = 39e^{-.00125c}$ mhos	13
5	Sponge Conductance of 30-mil Plaque Cycled on 6.25-Inch Arbor; $G = 30e^{-.00687c}$ mhos	14
6	Sponge Conductance of 30-mil Plaque Cycled on 7-Inch Arbor; $G = 36.7e^{-.00541c}$ mhos	15
7	Sponge Conductance of 30-mil Plaque Cycled on 8-Inch Arbor; $G = 37e^{-.00418c}$ mhos	16
8	Sponge Conductance of 30-mil Plaque Cycled on 9-Inch Arbor; $G = 25.4e^{-.00541c}$ mhos	17
9	Sponge Conductance of 30-mil Plaque Cycled on 10-Inch Arbor; $G = 47e^{-.00367c}$ mhos	18
10	Sponge Conductance of 40-mil Plaque Cycled on 9-Inch Arbor; $G = 100e^{-.00569c}$ mhos	19
11	Sponge Conductance of 40-mil Plaque Cycled on 10-Inch Arbor; $G = 90.8e^{-.00477c}$ mhos	20
12	Sponge Conductance of 40-mil Plaque Cycled on 13.75-Inch Arbor; $G = 31.7e^{-.00301c}$ mhos	21
13	Sponge Conductance of 40-mil Plaque Cycled on 20-Inch Arbor; $G = 31e^{-.00159c}$ mhos	22
14	Mechanical Parameter, ϕ, as a Function of Mean Strain ε	23
15	Schematic of Tensile Test Specimens	24
16	Load-Displacement Curve in Tension	25
17	Failure of Tensile Test Specimens	26
18	Resistance Change-Displacement Curve in Tension	27
19	Sponge Resistance Change-Displacement Curve in Tension	28
20	Sponge Resistance with Cyclic Tension at 2.5 Hertz	29

SECTION I
INTRODUCTION

In a recent paper (Reference 1) it has been shown that the mechanical fatigue characteristics of battery electrode plaque are related to the capacity retention characteristics of the active battery electrode. In general the distinction between the electrode plaque and the active electrode is as follows: the electrode plaque is the electrochemically inactive substrate in which the active chemical components are impregnated. A chemically impregnated plaque is an active battery electrode.

The work that has been reported on has been with sintered nickel plaque with NiOOH as the impregnate. This is the type of nickel electrode used in high quality, nickel-cadmium cells, nickel-zinc cells, and nickel-hydrogen cells. Air Force applications for these cells are primarily aircraft emergency power and spacecraft power. Thus, batteries with improved nickel electrodes are of some importance to the Air Force.

In this report some of the mechanical properties of nickel plaque are presented. The intent behind this work is to provide an initial data base for commercially available plaque. The key property is plaque electrical conductance and how it varies with cyclic mechanical strain. This data was taken by flexing the plaque over various diameter arbors, for c number of cycles, and periodically measuring the conductivity. In addition, the plaque was cyclically loaded in tension and the conductance continuously monitored.

The structure of the nickel plaque is substantially different than typical fatigue testing specimens. The plaque consists of a sintered nickel sponge, that is typically 90% porous, in which there is an internal nickel current collection screen; which is sintered to the sponge. The combination screen nickel sponge drops the overall plaque porosity to about 80%. It is the loss of sponge conductivity that is of particular interest.

The sponge material, without the screen, was found to be too fragile to handle for the test procedures used. For example, the attachment of the electrical leads would invariably damage the specimen. Thus, throughout this work it was necessary to use standard plaque and substract the effect of the screen. The procedures and assumptions made to do this are described as they are used within the report.

SECTION II
FATIGUE IN BENDING

To fatigue the plaque in bending it was flexed, in a compression-tension cycle, over various diameter arbors. The thickness (30 to 40 mils) of the plaque is much less then the arbor radiuses (2.75 inches to 10 inches) therefore the strain is bounded by the ratio of plaque thickness, t, over the arbor radius, r. This ratio is not the maximum strain as one has to account for the position and thickness of the nickel screen. In the test samples used the screen was visible on one side of the plaque, thus the expression for the mean strain, ε, becomes (Figure 1),

$$\varepsilon = \frac{t - d/2}{2r}$$

where d is the screen thickness and where it is assumed that the plane of zero strain is the center of the screen.

The resistance of the plaque is measured with a small AC test current. As the plaque fatigues the resistance increases due to the breaking of sintered bonds in the nickel sponge. It is assumed that the screen is a "non-fatiguing" element of the plaque. Thus, when the plaque fails it is reasonable to expect the resistance to be that of the nickel system. This does not occur because the screen does not shed the sponge, thus mechanical contact within the sponge (Figure 2) is maintained, providing a "high resistance" current path. The functional dependence of the sponge resistance on cycles and strain is assumed to be unaltered by the presence of the screen. This is reasonable when one considers the expected behavior of a plaque without a screen. The only expected difference with cycling, up to fracture, would be a lessening of the strain magnitude due to a shift in the plane of zero strain to the plaque centerline.

In Figure 3 resistance data versus cycles is shown for a typcial test. The resistance asymptote is determined by flexing the sample

over a 1.75 inch diameter arbor for one cycle. The asymptote is assumed, via previous discussion, to be the failure of the nickel sponge. Thus, on a conductance plot for the sponge the asymptote is the zero conductance point. Therefore, the reciprocal of the difference between the asymptotic resistance and the resistance at cycle c is the sponge conductance. In Figures 4 through 13 the conductance plots are shown for two plaque thicknesses and various arbor diameters. The solid line is a fit to the data using an expression of the form

$$K_o e^{-\phi c}$$

where K_o is the initial conductance, ϕ a parameter to be determined, and c the number of cycles. In general, this expression fits the data quite well and is the expression used in Reference 1 to describe the conductivity versus cycles relationship. The variation in the initial values of conductance is principally due to variations in sample size.

In Figure 14 ϕ versus the mean strain, ε , is shown. A point to note is that ϕ is initially linear in ε. This linearity extends over the range of ϕ's that were found during actual cell testing. Thus, it appears safe to assume that

$$\phi = a\varepsilon$$

when applying these results to a battery. In addition, the results for 30-mil and 40-mil plaque fall on the same line which implies ϕ is independent of plaque thickness.

SECTION III
TENSILE TESTS

The purpose of the tensile tests is primarily to demonstrate a direct correlation between strain and conductance. This was accomplished for both static and dynamic test conditions.

The tensile test specimens were fabricated from commercial 30-mil plaque according to Figure 15. A typical load-displacement curve is shown in Figure 16. From Figures 15 and 16 the plaque Modulus of Elasticity is found to be 1.51×10^5 lbs/in^2. For convenience a stiffness factor, k, is used where k is given by

$$\text{Load} = k\delta$$

where δ is the increased length due to loading. k is found to be 2060 lbs/in.

The crack structure in the failed specimens is shown in Figure 17. Note that the cracks do not extend much beyond the test section; therefore the geometry of the test specimen must be accounted for when determining the strain, ε , across the test section. It is readily determined that

$$\varepsilon = \frac{\delta}{2.20}$$

It appears, from test observation, that the sinter sponge provides negligible contribution to the stiffness of plaque loaded in tension. In addition, before and after measurements of the test specimens physical dimensions indicate that the Poisson's Ratio for the plaque can be taken to be zero. There was no measurable change in either the thickness or width of the plaque with increasing δ.

In Figure 18 the resistance versus displacement curve is shown for static test conditions. Note, the initial decrease in the resistance. This was caused by the test machine chucks putting a compressive load on the specimen when locking in position. Also, a slight buckling was

observed in the specimen at lock up. Therefore, zero displacement is taken as occurring at the minimum resistance value; where it is assumed the specimen starts tensile loading.

The resistance of the plaque can be viewed as two resistances in parallel. These being, the resistance of the nickel sponge, R_s, and the nickel screen, R_n. The value of R_n, for a one in^2 sample, is approximatley 6.125 milliohms. This was determined by measuring the resistance of similar screen. Denote the plaque resistance by R_p then

$$\frac{1}{R_p} = \frac{1}{R_s} + \frac{1}{R_n}$$

The values of R_p are taken from Figure 18 and R_n is given by

$$R_n \simeq \frac{6.125 m\Omega}{(1 - \sigma\varepsilon)^2}$$

where σ is Poisson's Ratio for nickel. The value of σ is 0.31 (Reference 2). Note, that σ is applied only to the screen which is fabricated from nickel wire. For the nickel sponge σ is zero.

The R_s versus δ curve is shown in Figure 19. Thus, under static conditions, it is seen that the nickel sponge resistance is a function of ε.

It is necessary to establish that the resistance-strain characteristics determined by static testing can be applied to dynamic situations. Such dynamic conditions occur in a battery during the charge-discharge cycles. These cycles are generally on the order of hours (thus, quasi-steady state) but under some conditions on the order of minutes. In the dynamic mechanical tests reported here the tensile machine was cycled at 2.5 Hertz. The minimum load was zero pounds and the maximum load was 16 pounds. The resulting resistance versus ωt is shown in Figure 20.

From the static testing data and the dynamic test conditions a calculated resistance-ωt curve can be obtained. From Figure 19 it is seen that R_s can be approximated by

$$R_s = 1.866e^{250\delta^2}$$

Let

$$\delta = \frac{16 \text{ lbs}}{2060 \text{ lbs/in}} \quad \frac{(1 + \sin\omega t)}{2}$$

Then

$$\frac{1}{Rp} = \frac{1}{1.866e.00378(1 + \sin\omega t)^2} + \frac{(1-.141\delta)^2}{6.125}$$

The above equation is the calculated curve in Figure 20.

The calculated curve and the test results are in qualitative agreement. There are several reasons that could contribute to the difference in the two curves. These are listed as follows:

a. The calculated results are sensitive to the zero offset of Figure 18. A reduced offset would give better agreement.

b. Resistivity differences between samples.

c. The tensile testing machine was operated at maximum sensitivity, and difficulty was experienced in estimating the dynamic test load and with sine wave distortion due to hydraulic noise.

d. Mechanical friction damping within the nickel sponge could limit displacement.

SECTION IV
CONCLUSIONS

The results of the tests done on nickel battery plaque has provided sufficient information to allow the following conclusions to be made:

a. The electrical conductivity of battery plaque is mechanical strain sensitive. For increasing strain the conductivity decreases.

b. Subjecting the plaque to cyclic strain results in permanent conductivity loss due to fatigue failure of the porous nickel sinter.

c. Results of this report plus Reference 1 indicates fatigue characteristics of nickel plaque are important to battery performance. The fatigue properties of the plaque may be an important quality control consideration.

d. Currently available fatigue testing equipment is not adequate for battery plaque testing. Special equipment that can apply small test loads is needed. It has not been established what is the best type of fatigue test but it has been found that bending fatigue gives meaningful results.

REFERENCES

1. D. Fritts, "The Determination of Porous Electrode Fatigue Properties Using Multigrid Electrodes", Eleventh International Power Sources Symposium, Brighton, England, 1978.

2. J.G. Thompson, "Nickel and Its Alloys", pg. 26, National Bureau of Standards Circular 592, February 5, 1958.

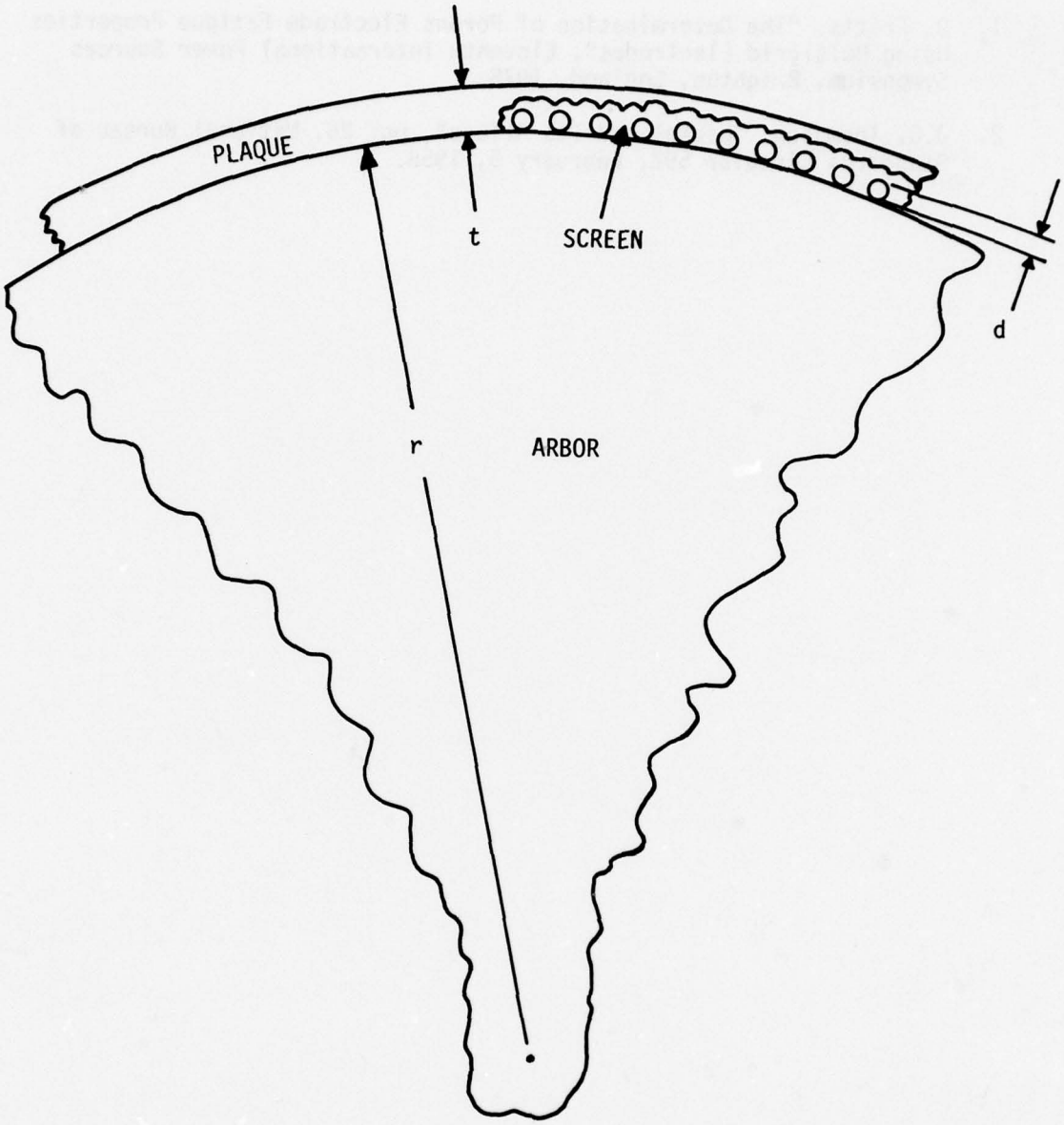

Figure 1. Fatigue Bonding Test

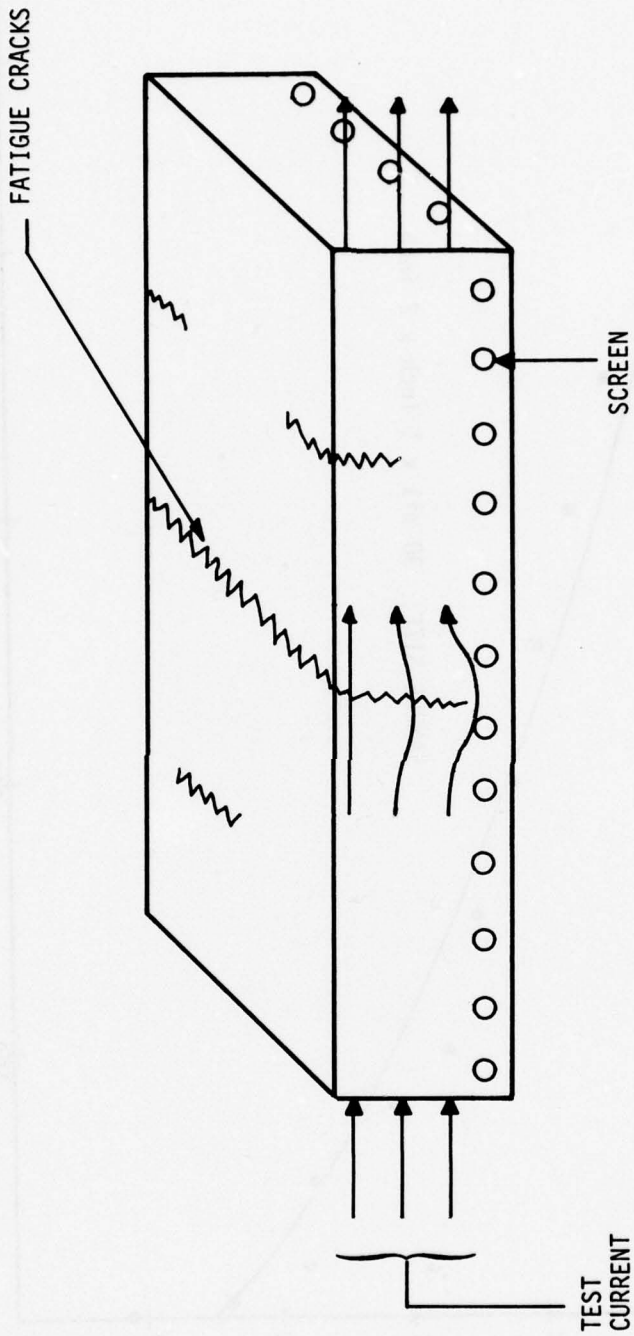

Figure 2. Schematic of Failed Specimen

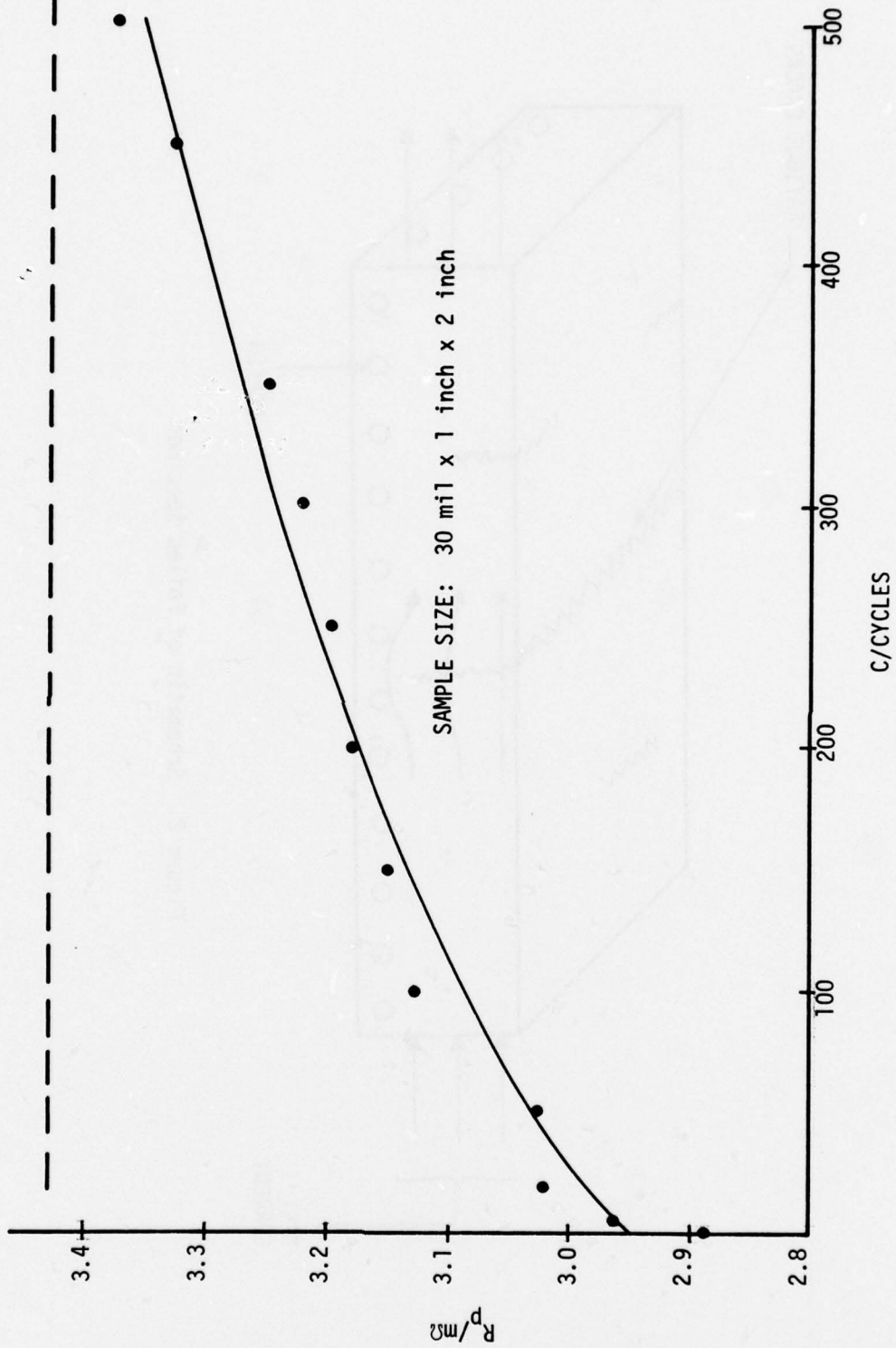

Figure 3. Characteristic Resistance Increase with Cyclic Bending

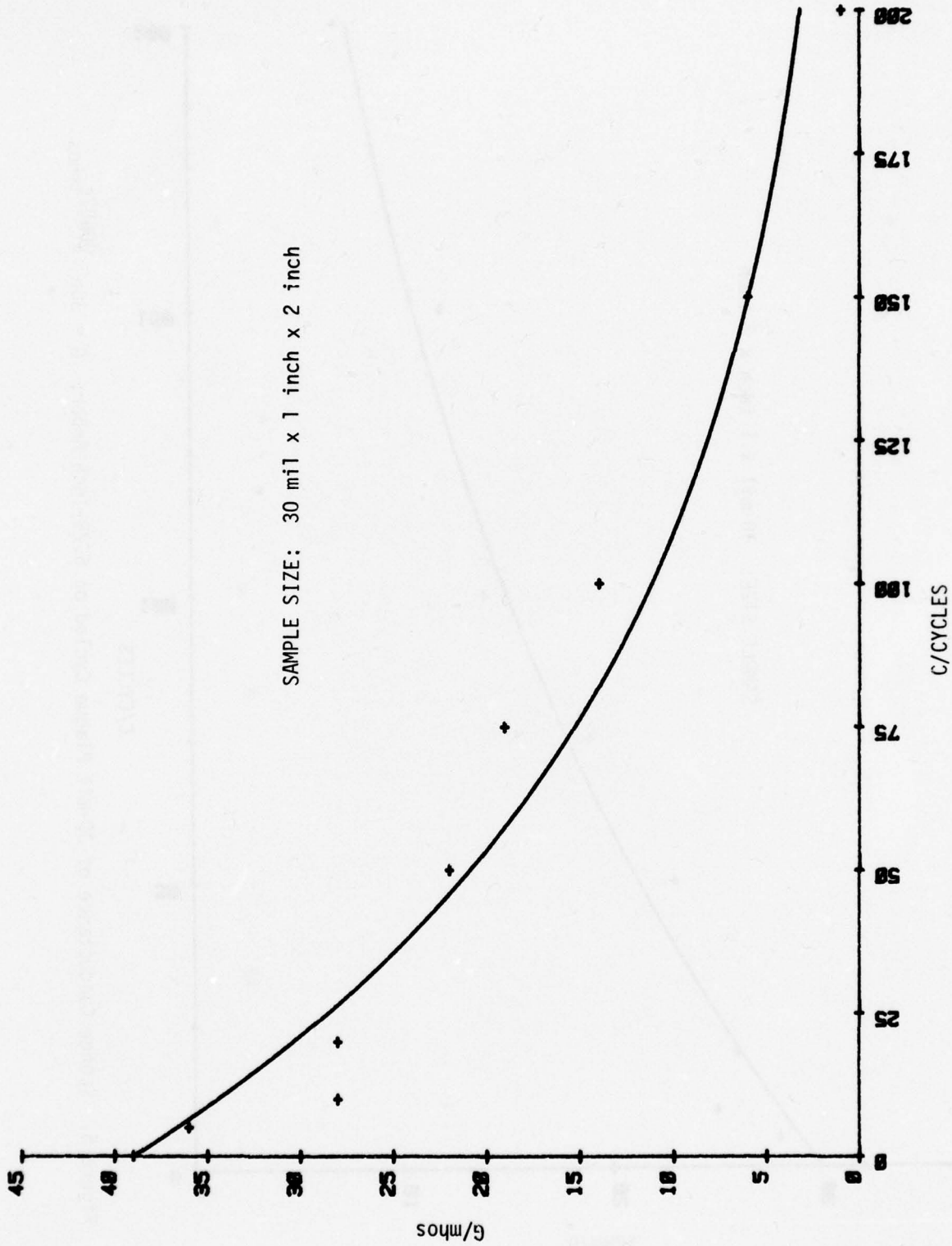

Figure 4. Sponge Conductance of 30-mil Plaque Cycled on 5.5-Inch Arbor; $G = 39e^{-.00125c}$ mhos

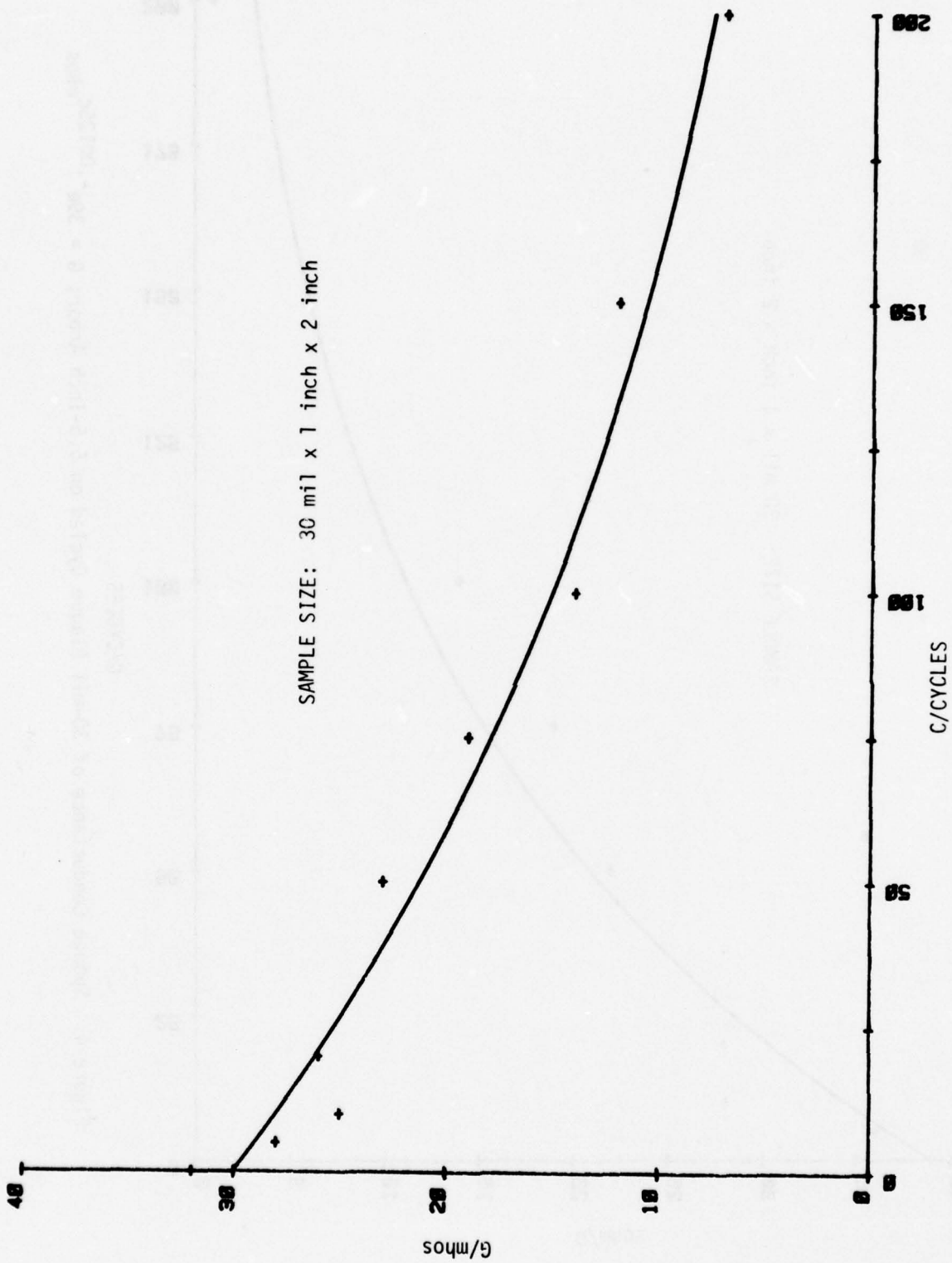

Figure 5. Sponge Conductance of 30-mil Plaque Cycled on 6.25-Inch Arbor; $G = 30e^{-.00687c}$ mhos

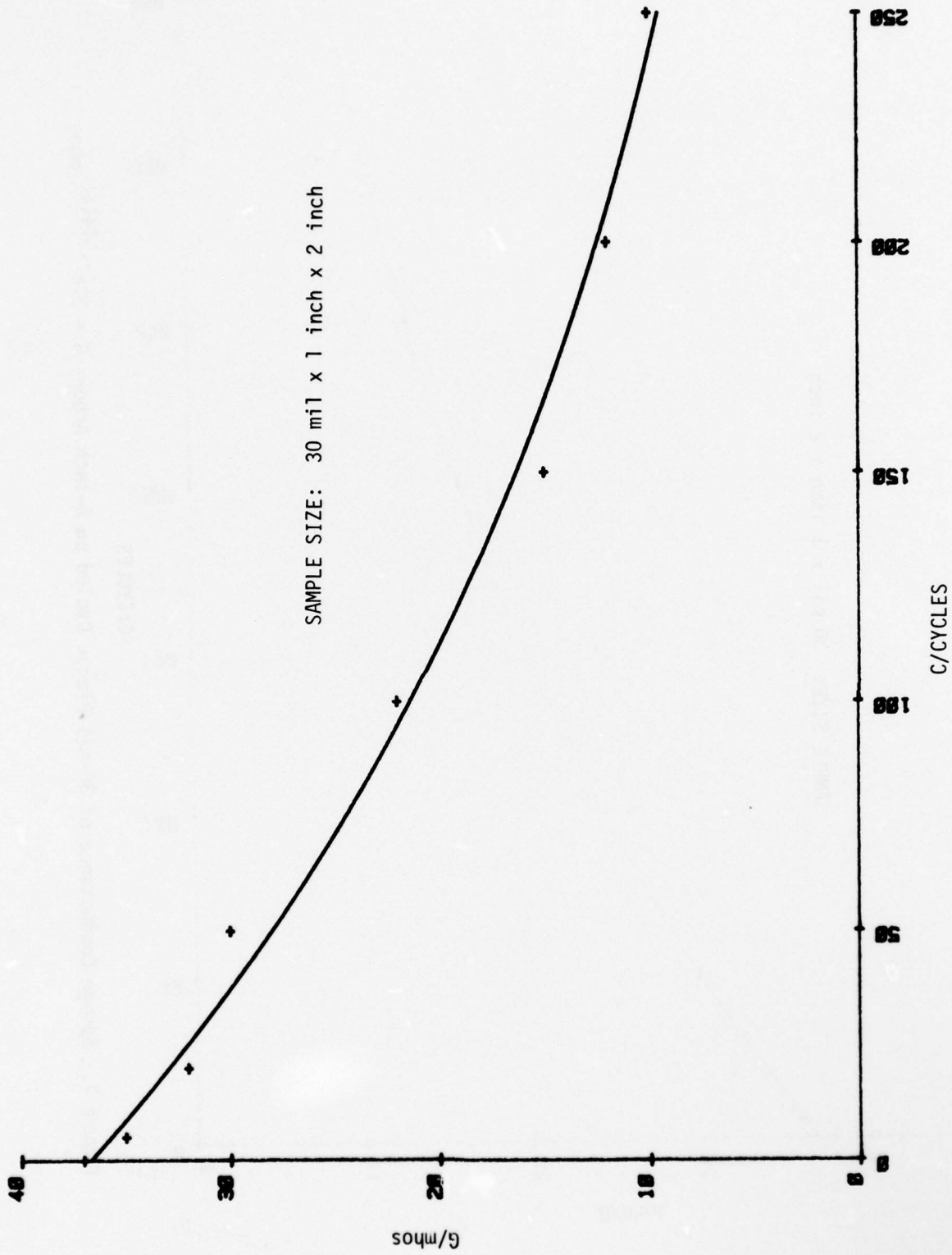

Figure 6. Conductance of 30-mil Plaque Cycled on 7-Inch Arbor; $G = 36.7e^{-.00541c}$ mhos

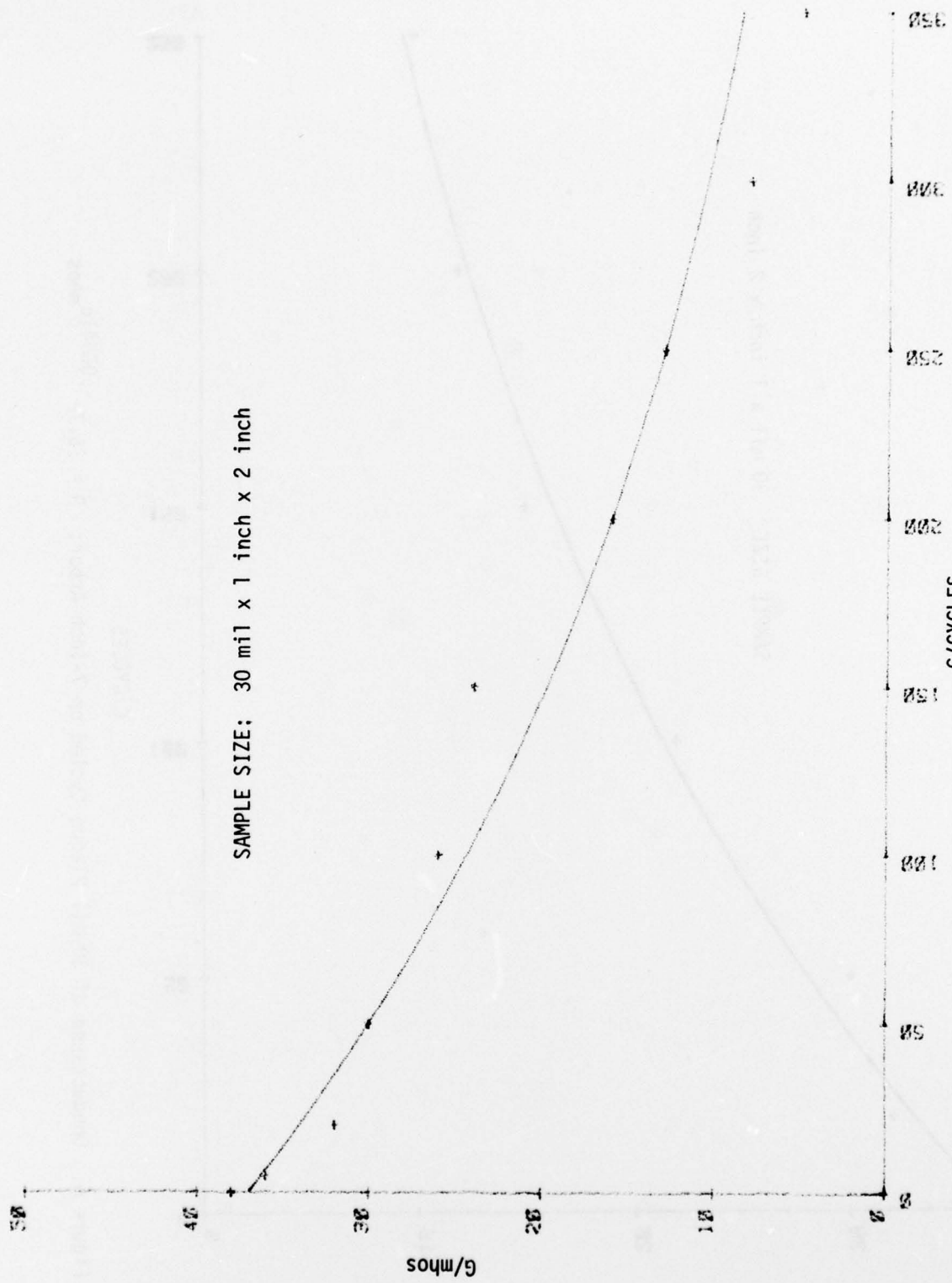

Figure 7. Sponge Conductance of 30-mil Plaque Cycled on 8-Inch Arbor; $G = 37e^{-.00418c}$ mhos

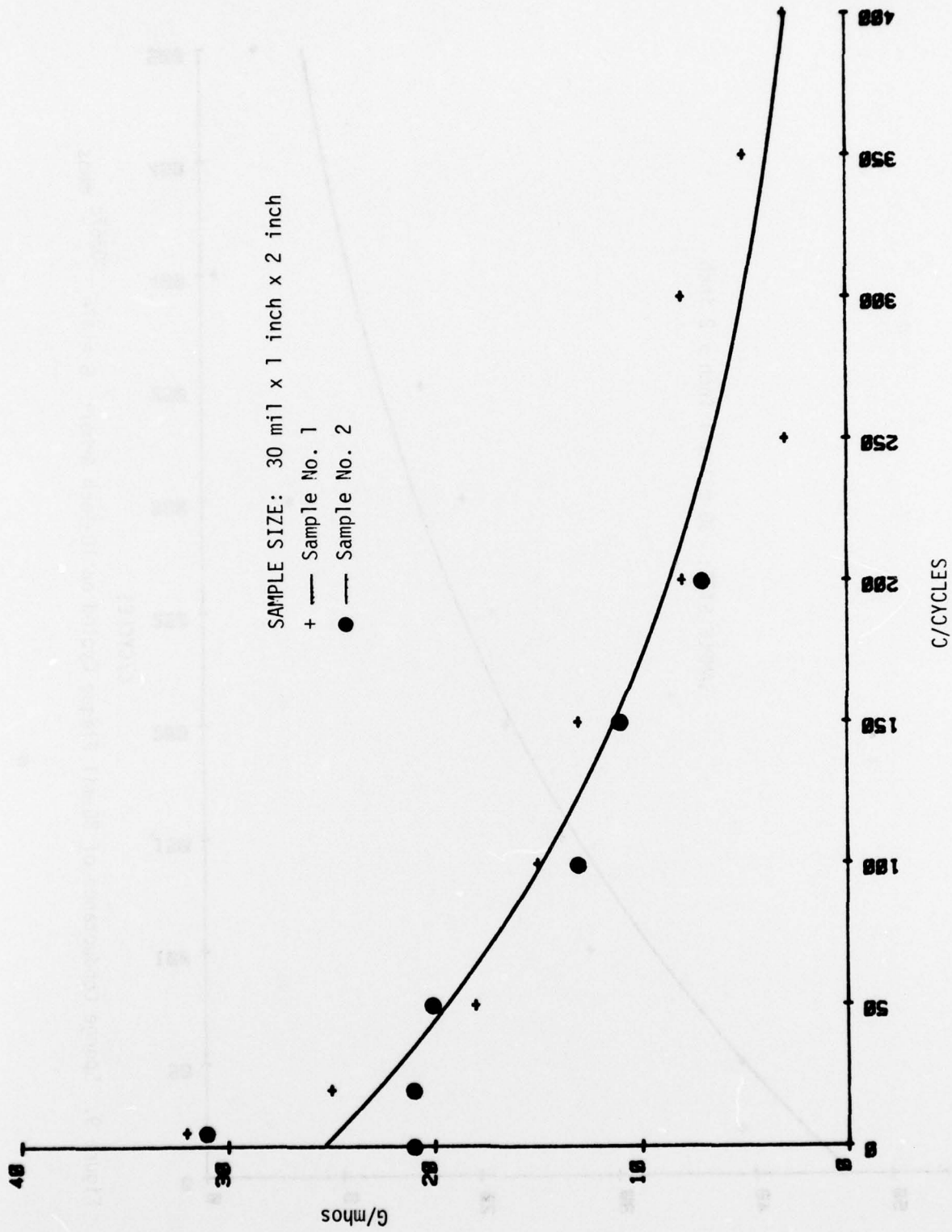

Figure 8. Sponge Conductance of 30-mil Plaque Cycled on 9-Inch Arbor; $G = 25.4e^{-.00541c}$ mhos

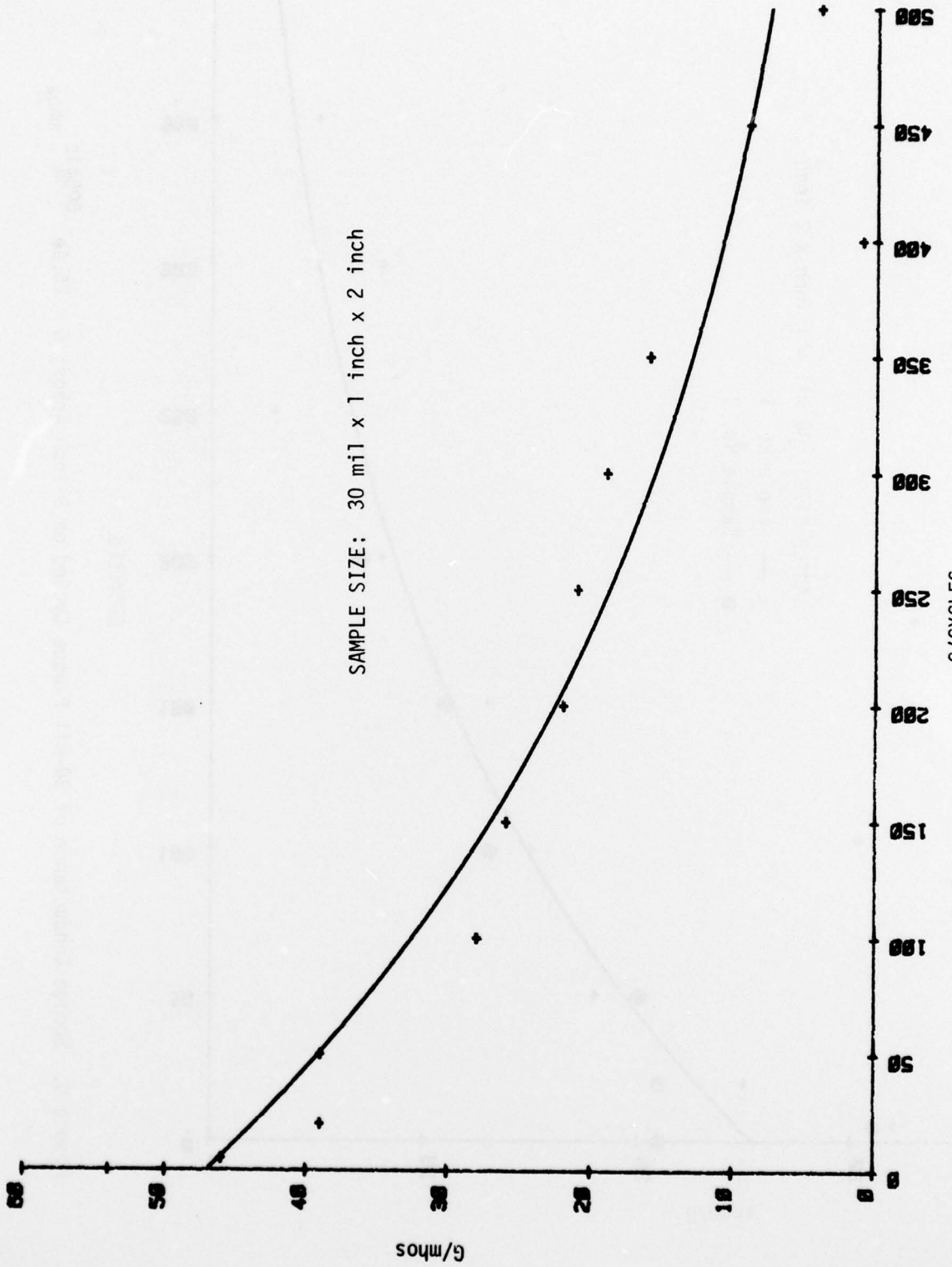

Figure 9. Sponge Conductance of 30-mil Plaque Cycled on 10-Inch Arbor; $G = 47e^{-.00367c}$ mhos

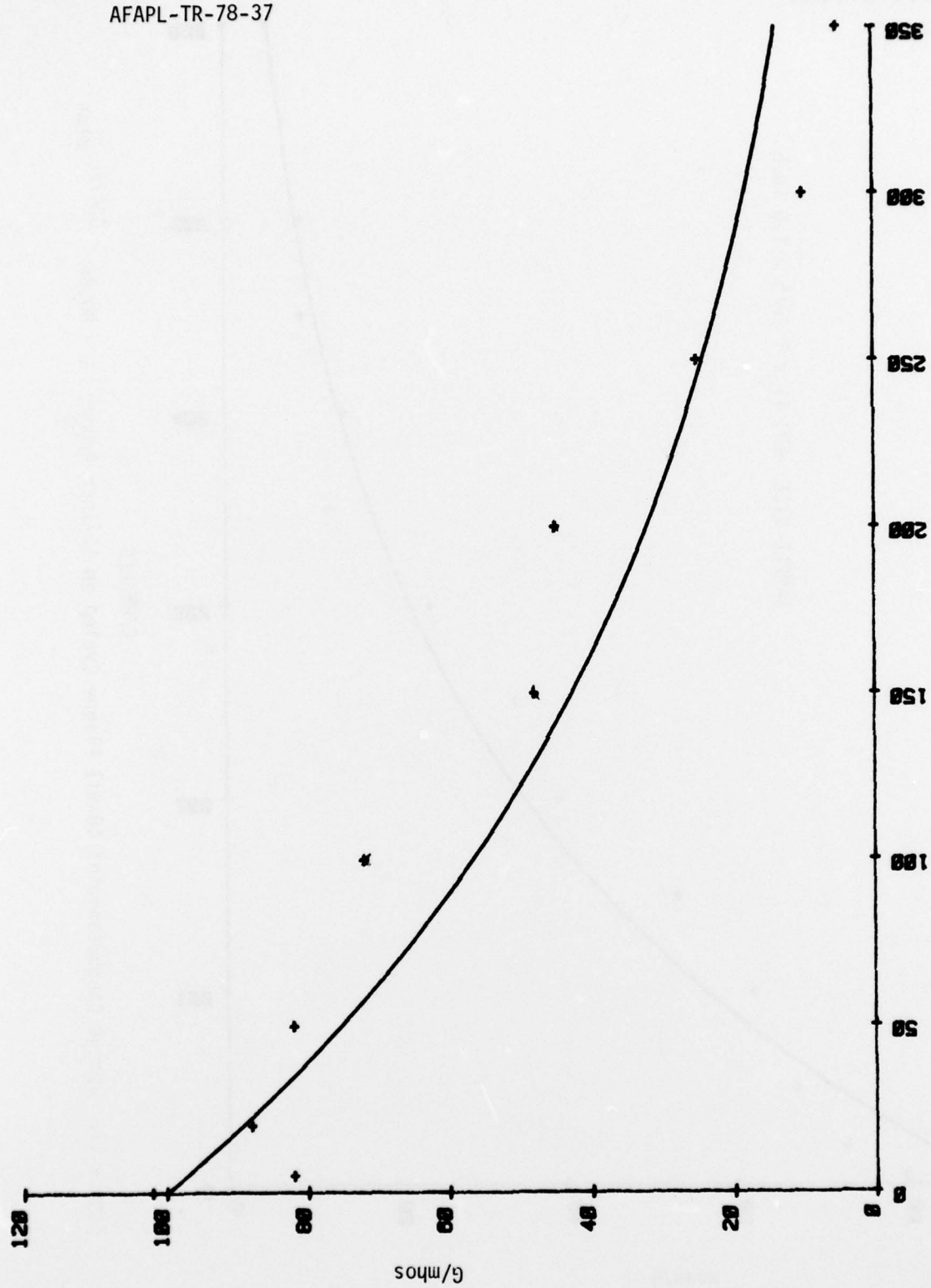

Figure 10. Sponge Conductance of 40-mil Plaque Cycled on 9-Inch Arbor; $G = 100e^{-.00569c}$ mhos

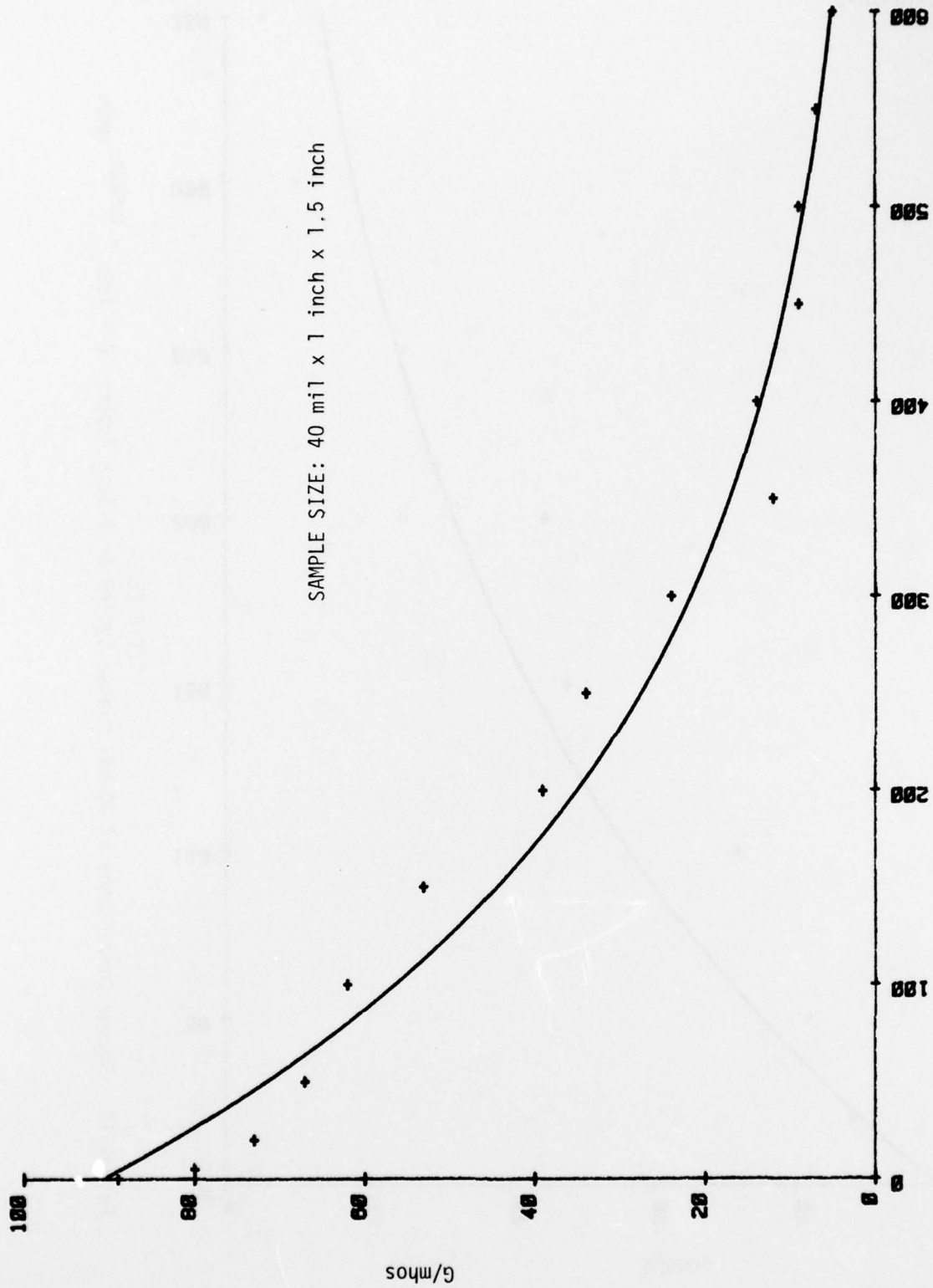

Figure 11. Sponge Conductance of 40-mil Plaque Cycled on 10-Inch Arbor; $G = 90.8e^{-.00477c}$ mhos

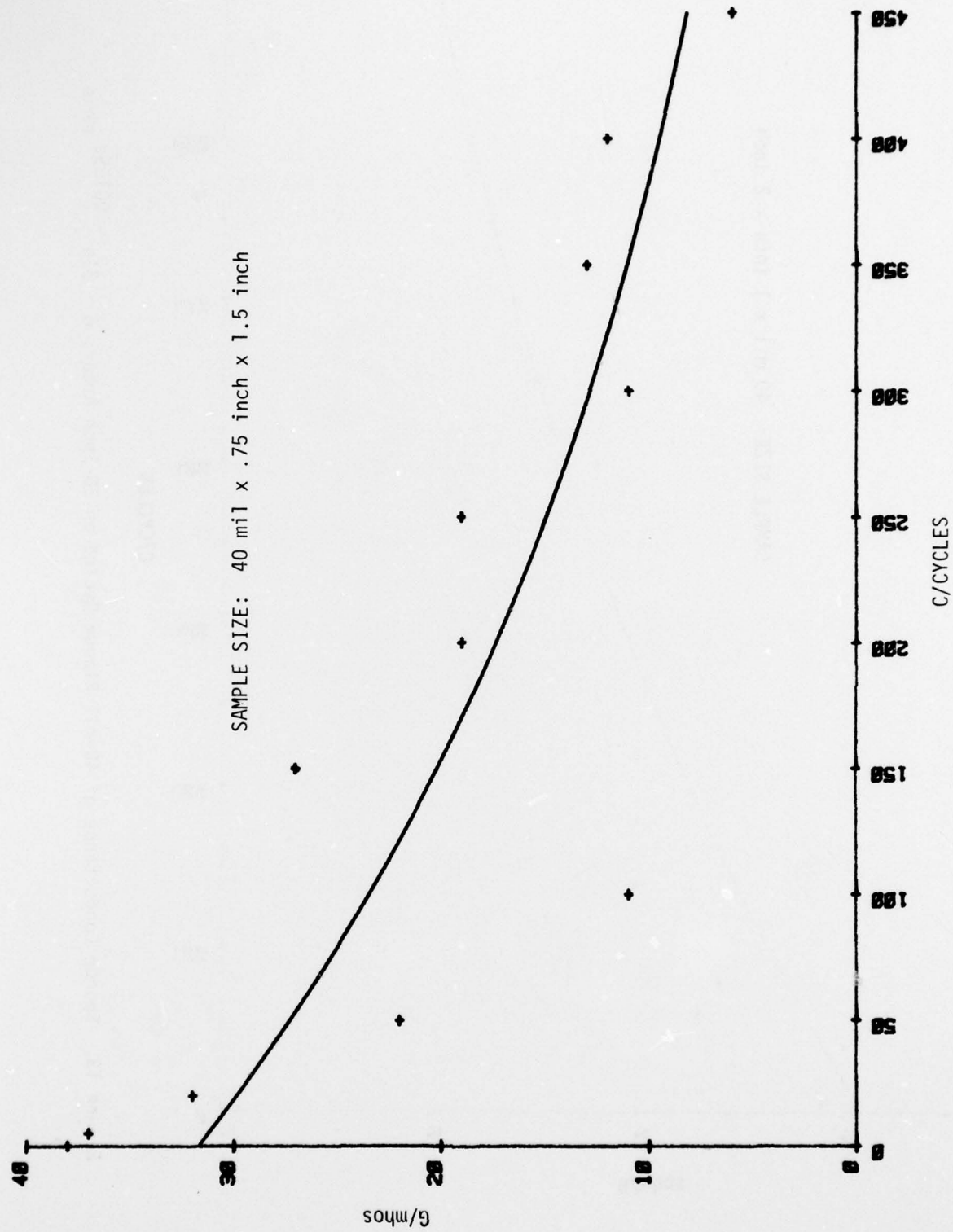

Figure 12. Sponge Conductance of 40-mil Plaque Cycled on 13.75-Inch Arbor; $G = 31.7e^{-.00301c}$ mhos

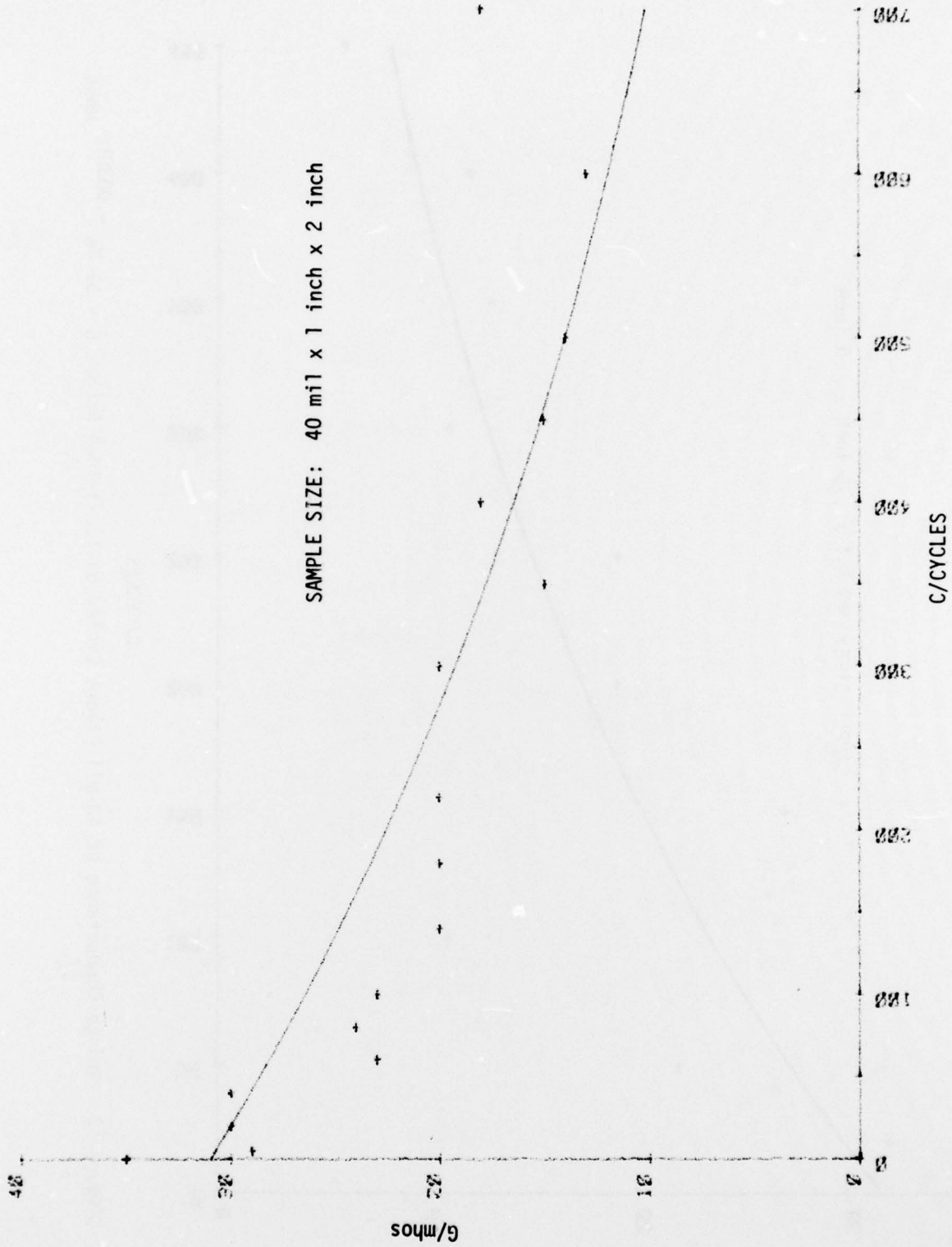

Figure 13. Sponge Conductance of 40-mil Plaque Cycled on 20-Inch Arbor; $G = 31e^{-.00159c}$ mhos

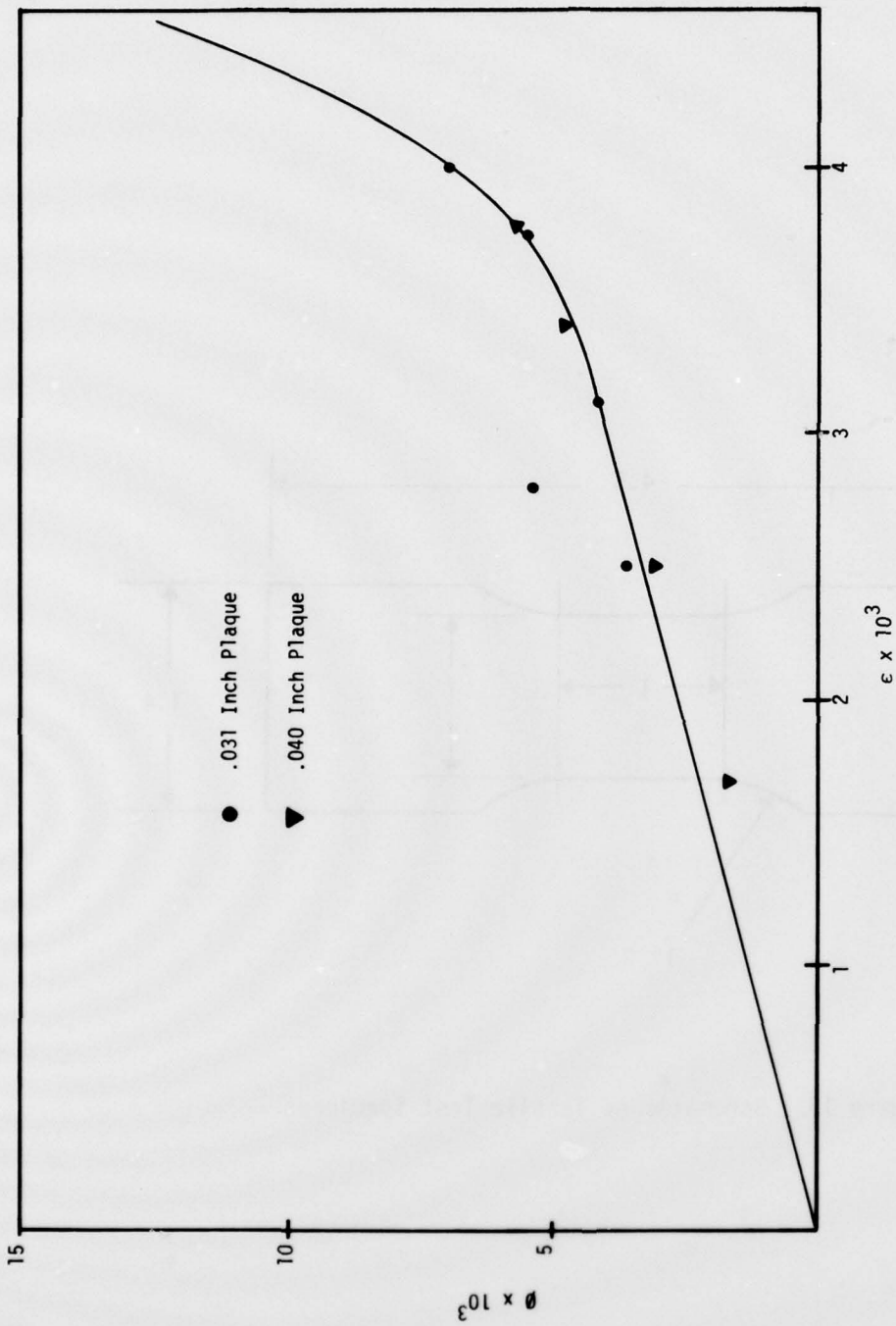

Figure 14. Mechanical Parameter, ϕ , as a Function of Mean Strain, ε

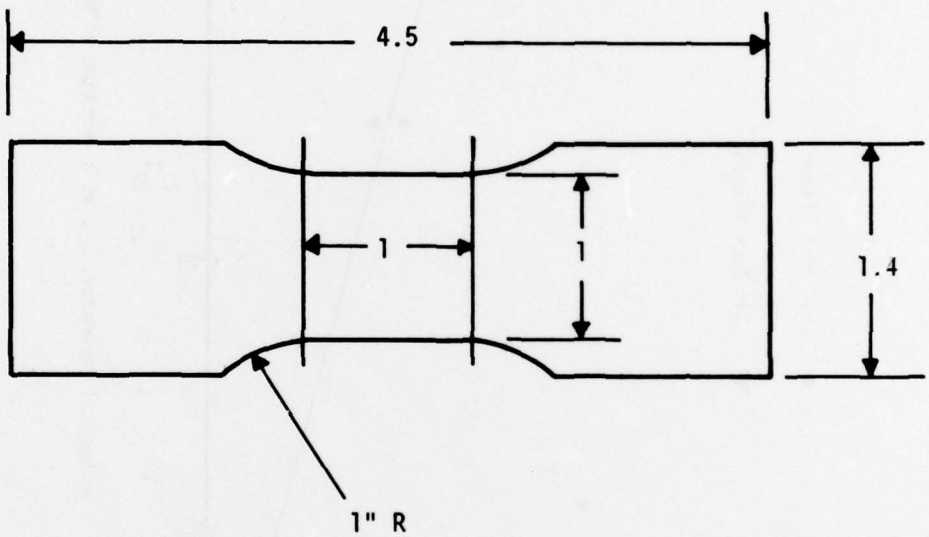

Figure 15. Schematic of Tensile Test Specimens

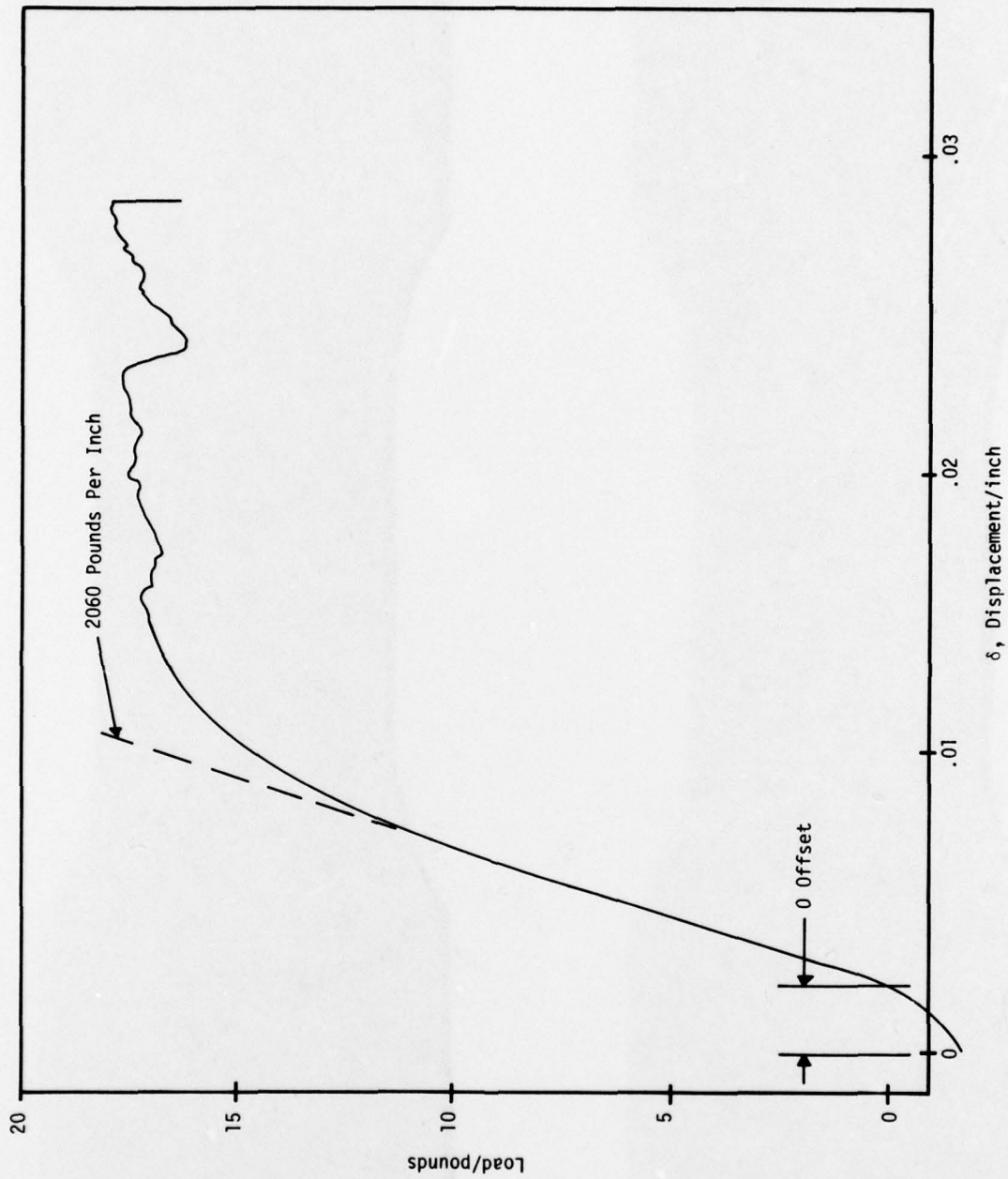

Figure 16. Load-Displacement Curve in Tension

Figure 17. Failure of Tensile Test Specimens

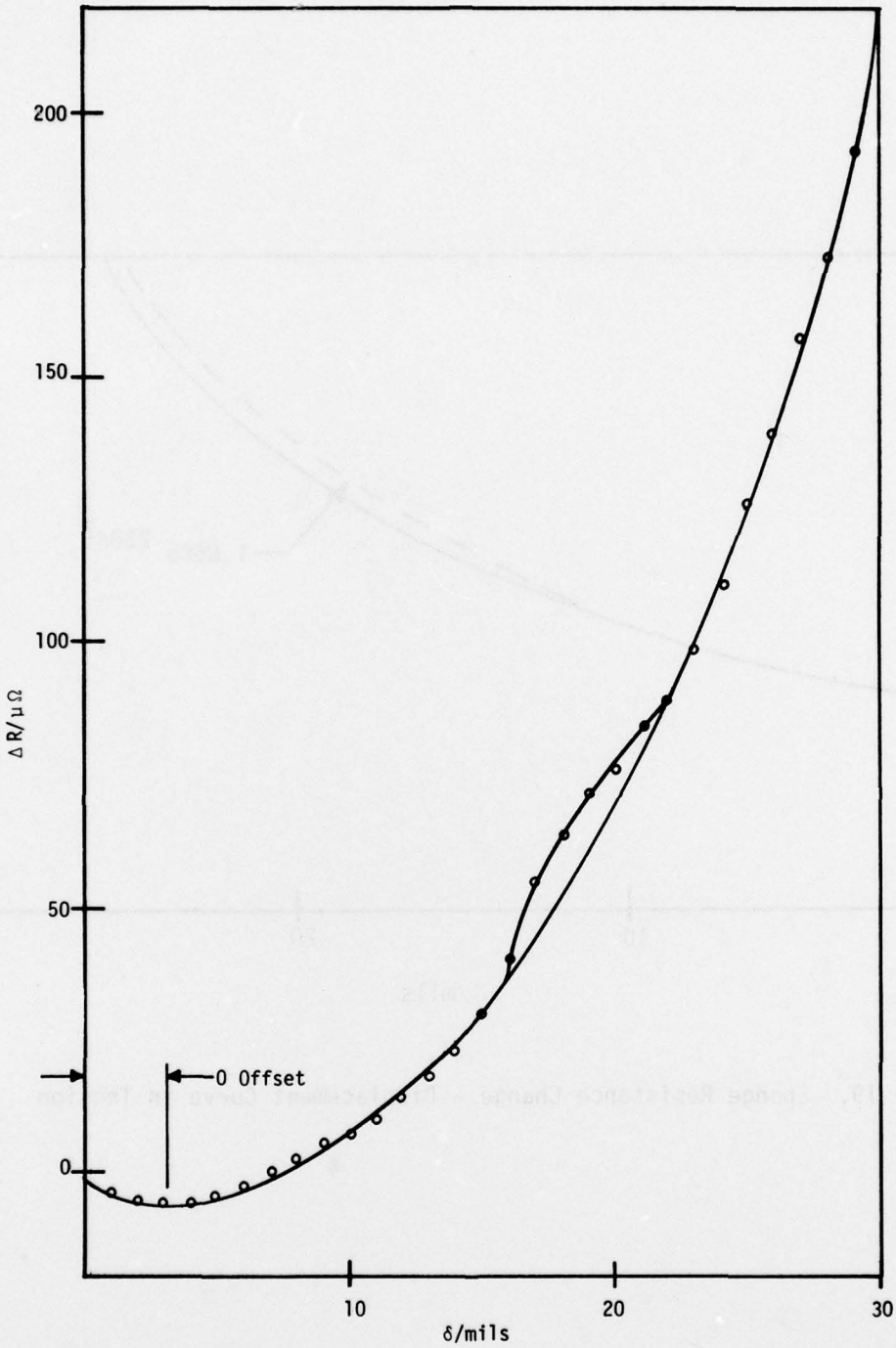

Figure 18. Resistance Change - Displacement Curve in Tension

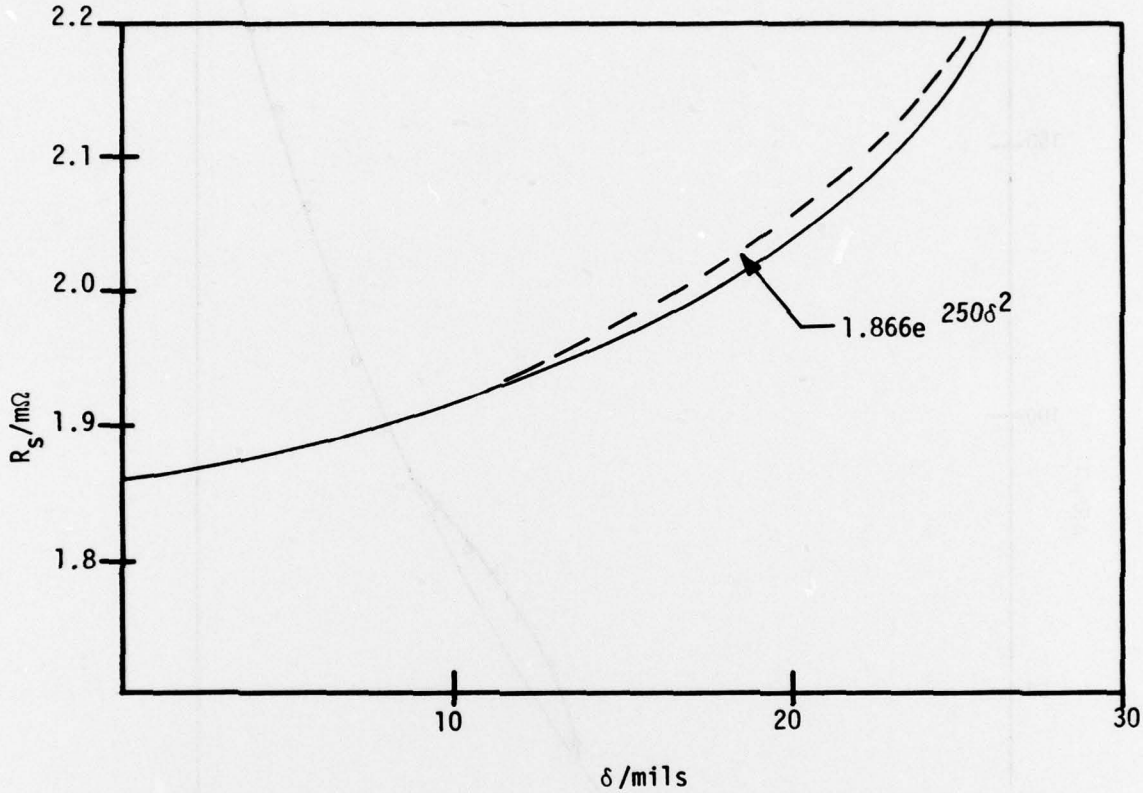

Figure 19. Sponge Resistance Change - Displacement Curve in Tension

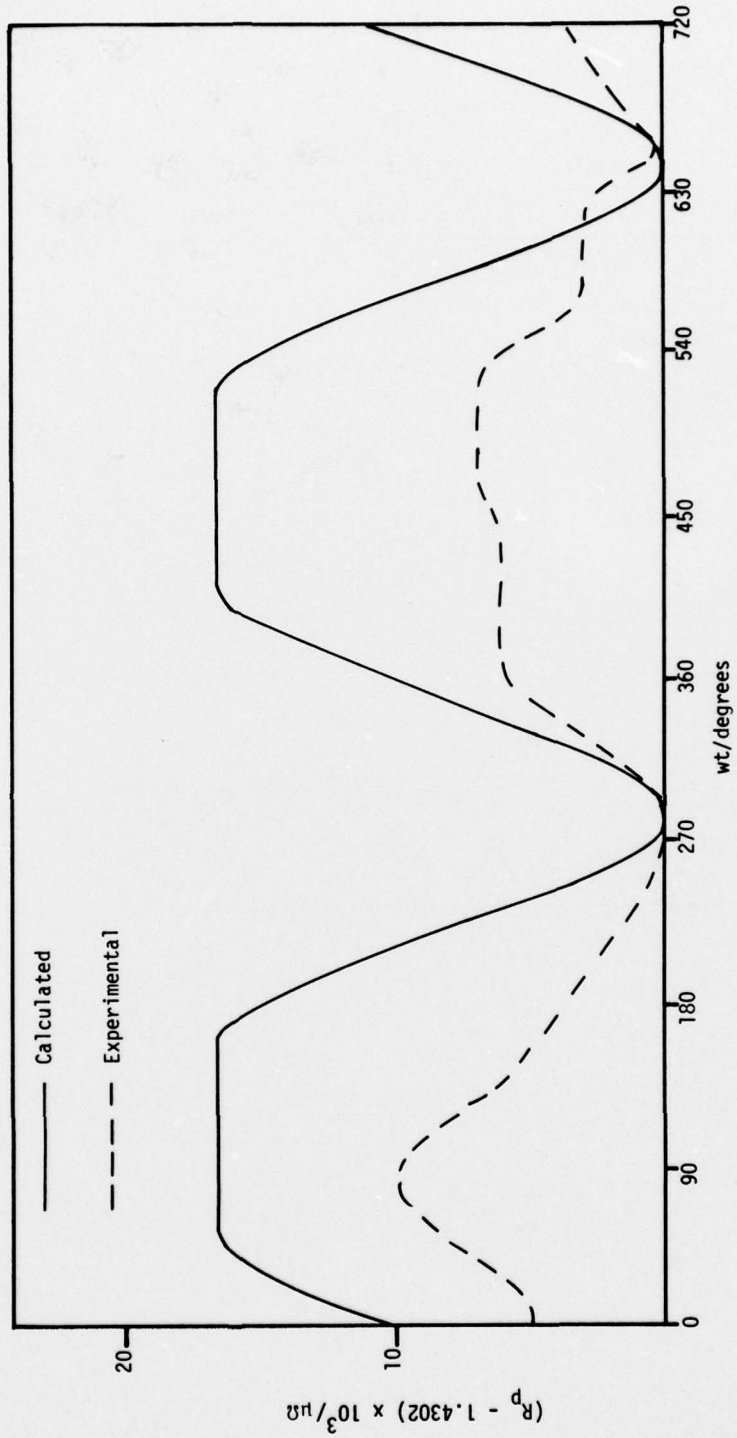

Figure 20. Sponge Resistance with Cyclic Tension at 2.5 Hertz

☆U.S.Government Printing Office: 1978 — 757-080/114